

Article

# Enhancing the Punching Load Capacity of Reinforced Concrete Slabs Using an External Epoxy-Steel Wire Mesh Composite

Abdulkhaliq A. Jafer , Raid AL-Shadidi and Saba L. Kareem \*

Civil engineering Department, College of Engineering, University of Misan, Maysan 62001, Iraq

\* Correspondence: sa.alkaabi12555@gmail.com or saba94@uomisan.edu.iq

Received: 22 June 2019; Accepted: 22 July 2019; Published: 24 July 2019



**Abstract:** The present experimental work investigates the applicability and performance of a new strengthening method for concrete slabs, intended to increase their punching resistance using combination layers of steel wire mesh with epoxy attached to the concrete slabs' tension face. Six simply supported square reinforced concrete slab specimens were tested up to failure under a central concentrated load. The main parameters in the study are the concrete compressive strength (30 MPa and 65 MPa) and the configuration of a bundle externally fixed to the tension side of the tested slabs. The experimental results appeared to greatly enhance the performance of the specimens, as they were externally strengthened under this new method. When compared to the control slabs, the punching load and stiffness of the strengthened slabs increased up to 28% and 21%, respectively.

**Keywords:** epoxy; ferrocement; flat slab; punching shear; wire mesh; ductility

## 1. Introduction

Flat slabs are one of the more common types of slabs used in concrete construction, such as office buildings, warehouses, and car parks. This system consists of columns and slabs only, without beams, drop panels, or column capitals. In addition to cost savings and reduced construction time, the main advantage of this system is that it provides a clear height of building spaces, which facilitates the erection of the building services equipment with no restrictions in floor space partitioning.

The failures of flat slabs occur either due to flexure or punching. Flexure failure occurs when the amount of steel reinforcements located at the tension side of the flat slab are relatively little and the yielding of the reinforcement governs the strength of the specimen [1]. When the high main reinforcement ratio is used, the punching failure of concrete slabs occur at the region of connection between the slab and the column. The punching shear failure is characterized by the main steel reinforcement does not reach the yielding strain when the concrete is in the vicinity of the column, as it reaches the crushing stage [2,3]. It takes place suddenly, without any warning and with small displacement, resulting in a brittle mode failure. This leads to the progressive failure of the flat slab structure. Punching shear failure has a critical impact on structural engineering systems and thus should be avoided.

However, strengthening, rehabilitating, and repairing existing concrete structures are all successful methods for upgrading and improving the carrying capacity and extending service life of slabs. These methods become necessary due to changes in building usage, structural alterations, correcting for an error in the design or construction, constrain cracking, or when overloading occurs [4,5]. The decision for choosing a suitable strengthening technique is dependent on varied parameters, such as the structural efficiency, overall cost, and period of application [6].

A number of strengthening techniques have been developed to improve the serviceability and strength of concrete flat slabs. The traditional techniques for strengthening concrete flat slabs is to avoid abrupt punching shear failure, comprise and utilize steel plates linked to concrete slab with bolts or epoxy, externalize post-tensioning reinforcement, and increase the slab thickness in the region vicinity of column. These methods have been proven to be active in increasing the cracks and ultimate load and deformation capacities of slab-column joints [7–12]. In total, these methods have enhanced the performance of strengthened structures.

The main disadvantages of using steel plates are the high density of steel, aesthetic appearance, and corrosion problems [4,13]. In order to overcome these problems, fiber reinforced polymer (FRP) has been used. FRP exhibits several engaging properties, like a lower ratio of weight relative to strength, high durability, and simplicity of the installation [14–18]. Improvements in the shear characteristics of strengthened slab-column connections using FRP sheets have been previously reported [19–23]. Wang carried out an experimental study for predicting the shear capacity of strengthened central slab-column joints with carbon fiber reinforced polymer (CFRP). Four slabs (1750 mm square and 120 mm thick) with a central column stub (150 × 150 mm) were constructed and tested to failure. The CFRP strips were placed nearby to the face of the column in orthogonal directions at the soffit of slabs. The results illustrated that the punching shear strength of strengthening slab-column connections with CFRP sheets had a slight increase with an average of 8% than the reference slab [24]. Sharaf et al. conducted an experimental program to figure out the punching shear capacity of flat slabs externally reinforced with CFRP sheets. They constructed six full-scale slab column connections of 150 mm thick and 2000 mm square slab. The main parameters of their study included the configuration and amount of CFRP reinforcements. Their test results showed that the punching load of strengthened slabs increased between 6% and 16% greater than that of the reference slab [25]. Soudki et al. explored the behavior of concrete slabs externally reinforced by CFRP strips and subjected to punching load. Six slabs with dimensions of (1220 mm × 1220 mm × 100 mm) and square column (150 × 150 mm) were used. All specimens were simply supported along their edges and reinforced with same amount in each direction and tested under a monotonic punching load up to failure. The experimental results demonstrated that the strengthened slabs have a higher ultimate punching capacity than the control specimen (29%) [26]. The effect of using multiple layers of CFRP sheets as an external strengthening technique for two-way slab-column connections was investigated by Harajli and Soudki. The test program consisted of 16 square specimens with dimensions of 670 × 670 mm and different thicknesses of slabs (55 and 75 mm). The internal reinforcement used was placed in the tension side of the slab in perpendicular directions with two ratios (1% and 1.5%). One and two layers of CFRP sheets were bonded on tension or in tension of the compression sides of slab and then placed in the same directions of internal reinforcement. The test results revealed that the best achievement when using one layer at the tension side of the slab and no significant improvement was observed for multiple layers on the compression side [21].

However, the major obstacle to FRP strengthening is premature debonding failure and the reduction in ductility of the FRP-strengthened reinforced concrete structures [27–31]. Anchorage of FRP reinforcement is an attractive technical solution to overcome such problems [32–36]. The performance of the anchorage system is mainly dependent on detailing and the installation process of the system. Moreover, the innovative techniques focused on the possibility of using textile reinforced mortar (TRM) or high-performance fiber reinforced cementitious composites (HPFRCC) materials for repairing RC slabs was achieved [37,38]. It was found that these methods can significantly enhance the performance of repaired specimens. Therefore, it may be utilized to successfully restore the incompetence of damaged specimens.

Ferrocement is a thin structural member produced by a special type of reinforced concrete in which the reinforcements are constructed of multiple layers of small wire meshes embedded into a hydraulic cement mortar [39]. Ferrocement has taken a prominent place among the other components used for construction, strengthening, and rehabilitation, due to the availability of raw materials and

because it can be fabricated in complex shapes with less skilled labor [40]. In addition, it displays a high ratio of tensile strength relative to its weight and possesses a better cracking distribution than traditional RC. Hence, it may be utilized in several practical applications for strengthening reinforced concrete (RC) members [6,41–52]. In general, the elements strengthened with ferrocement laminates provides significant enhancements in cracking, stiffness, and strength. However, the debonding problem between the ferrocement laminates and the strengthened members is the main drawback of using this technique in the strengthening process. However, strengthening via ferrocement consumes more time, allowing the mortar to gain ultimate strength. Therefore, one of the important challenges facing engineers is research about new materials and technologies requiring less time for construction and curing. Li et al. [53] studied the possibility of a rapidly strengthened method that consists of resin concrete and steel mesh for strengthening RC columns. The results showed that the resin concrete combined with the steel mesh was an effective method for strengthening RC columns and can be used in rapid strengthening.

Moreover, the technique developed by Qeshta et al. [54–56] was used to prevent the separation of the ferrocement composite. This method consists of wire mesh embedded in epoxy resin instead of cement mortar. It was found that the bond between the beams and the new composite has good flexural capacity, ductility, and energy absorption.

Some researchers worked on the strengthening of concrete members, i.e., beam elements using the wire mesh-epoxy composite technique to resist the flexure failures. However, there is no research regarding flat slabs strengthening using the wire mesh-epoxy composite technique. The advantages of using the composite of steel wires with epoxy adhesive as a desirable strengthening material are plentiful, as the method is easy and rapid in installation. Further, the method does not disturb the clear height room of the space. Additionally, it is durable and has good resistance to the corrosion. Therefore, further studies are needed to understand the behavior of different concrete elements such as slabs and the influence of certain parameters on the ultimate carrying capacity and failure modes of the strengthened flat slab using this technique. The purpose of this study was to assess the effectiveness of using wire mesh composite with an epoxy adhesive application method to strengthen reinforced concrete flat slabs against punching loads. Further, the study was intended to explore the influences of concrete compressive strength and the configuration of a bundle externally fixed to the slabs on the punching load carrying capacity of the strengthened slabs. In an attempt to achieve the aims of the research, six RC flat slabs, divided into two groups of strengthening slabs, were tested.

## 2. Experimental Investigation

The experiment presented in this paper consisted of testing six specimens that could aid in evaluating the results of enhancing the punching shear load capacity of RC slabs after strengthening them with an external epoxy-steel wire mesh composite. The main parameters investigated in this study included concrete compressive strength and the configuration of a bundle of steel wire mesh with epoxy resin that was externally fixed to the tension side of the tested slabs. The dimensions of the cast slabs were  $800 \times 800 \times 95$  mm. The tested specimens were divided into two groups: normal (N) strength concrete and high (H) strength concrete, respectively. Two of the N and H slabs were used as control specimens. The remaining four slabs were strengthened using a new technique that consisted of a steel wire mesh-epoxy composite for both types of concrete. Three of the four slabs—denoted as NP0.5, NP1.5, and HP 1.5—were strengthened with bands located at a distance equal to  $0.5 d$  and  $1.5 d$  from the column face and parallel to the column face (where  $d$  is the effective depth of the slab). The fourth slab—denoted as NS—was strengthened with bands located at the column's corners and parallel to the diagonals of the column. The details of the specimens and the major study variables are summarized in Figure 1 and Table 1. The crack patterns, the deflection occurred during the cracking and ultimate load, maximum deflection, and load-deflection curves were recorded throughout the test. All the slabs were a square in shape with 800 mm side length and 95 mm thick. They were reinforced using 10 mm diameter mild steel deformed bars spaced 95 mm in both directions. The reinforcement

was placed at the opposite side of the applied load with a clear cover of 20 mm to give an average steel ratio of  $\rho = 1.15\%$ .

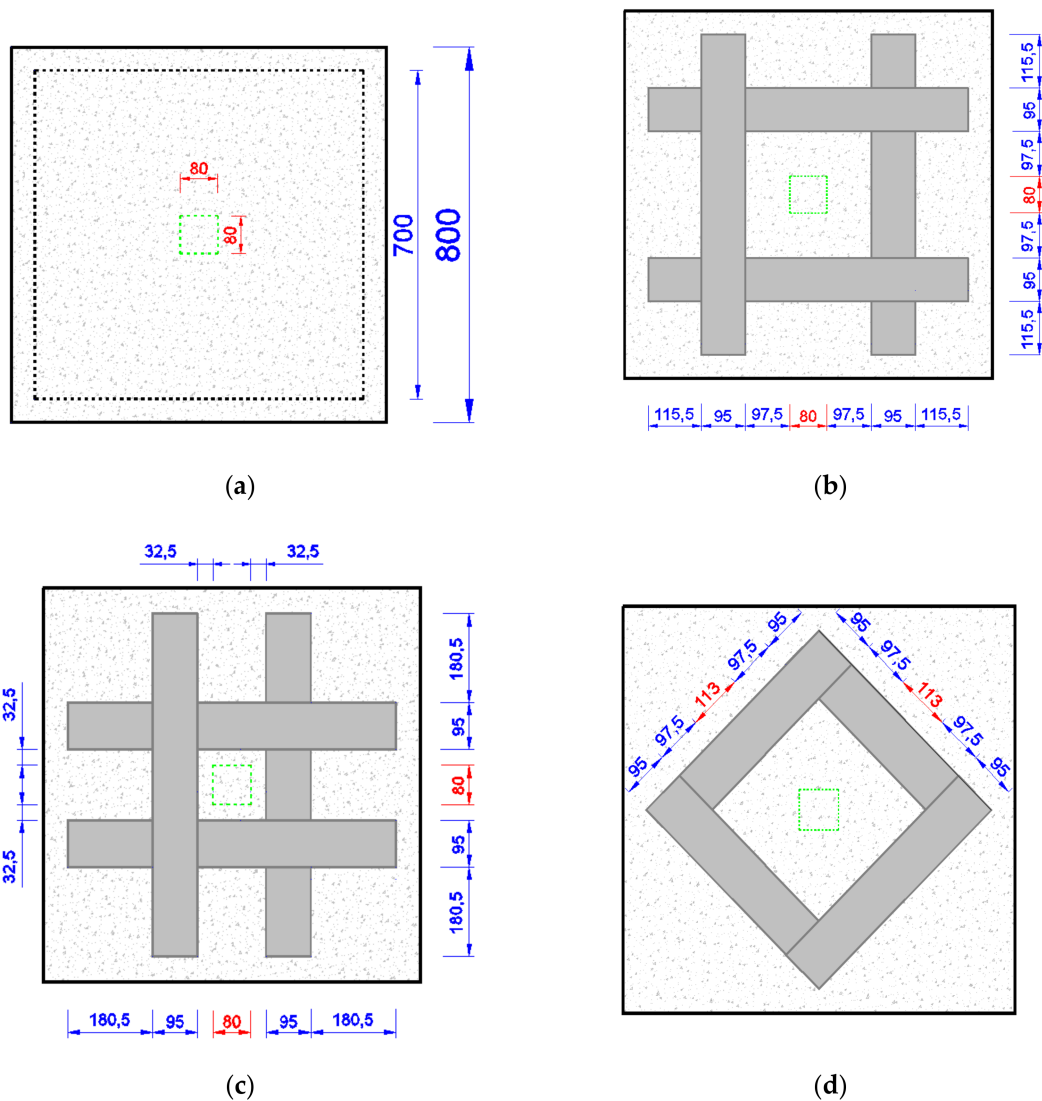


**Figure 1.** Schematic drawing showing wire mesh epoxy composite layout for specimens (unit: mm): (a) Control specimen N or H; (b) strengthened specimen NP 1.5 or HP 1.5; (c) strengthened specimen NP 0.5; (d) strengthened specimen NS 1.5.

**Table 1.** Details of specimens <sup>a</sup>.

Slab No.	Concrete Compressive Strength (MPa)	Strengthening Configuration
N	30	—
NP 0.5	30	Parallel to the column face and at 0.5 d from column's face
NP 1.5	30	Parallel to the column face and at 1.5 d from column's face
NS 1.5	30	Parallel to diagonals and at 1.5 d from column's corner
H	65	—
HP 1.5	65	Parallel to the column face and at 1.5 d from column's face

<sup>a</sup> d = Depth of the slab.

### 2.1. Concrete

In this study, the concrete used was made of Portland cement type I, which complies with the Iraqi Standard No. 5/1984 [57]. The specific gravity of the coarse and fine aggregate was 2.65 and 2.66, respectively; the fineness modulus of the fine aggregate was 3. Modified polycarboxylate-based polymer superplasticizer admixture in a dose of 2.25% by weight of cement and was added by mixing water, which achieved the required workability for high strength concrete. According to ACI committee 211 [58,59], the quantities of concrete ingredients are listed in Table 2, giving the average compressive and tensile strengths of concrete of each type, as shown in Table 3.

Table 2. Properties of concrete mix.

Concrete Type	Cement Content (kg/m <sup>3</sup> )	Coarse Aggregate (kg/m <sup>3</sup> )	Fine Aggregate (kg/m <sup>3</sup> )	Water/Cement	Superplasticizer (L/m <sup>3</sup> )
N	325	1150	650	0.5	-
H	530	950	680	0.3	12

Table 3. Properties of hardened concrete.

Concrete Type	Compressive Strength * (MPa)	Tensile Strength (MPa)
N	30	3.3
H	65	7.0

\* average of six specimens.

### 2.2. Steel Reinforcement

Deformed steel bars of 10 mm were used to reinforce the slab specimens. The average of three tensile test results is shown in Table 4 and compared with the relevant limits of ASTM standards [60].

Table 4. Mechanical properties of reinforcing steel.

Bar Size (mm)	Test Results			ASTM A615M		
	Yield Stress (MPa)	Ultimate Strength (MPa)	Elongation%	Yield Stress (MPa)	Ultimate Strength (MPa)	Elongation %
10	510	657	13.9	420	620	9

### 2.3. Steel Wire Mesh

Steel wire mesh with a welded square opening of 12.5 mm side length and an average diameter of 1.0 mm was used in this study. Three tensile coupons of wire mesh were tested under direct tension using a 5 kN capacity Bench-Top testing machine (model BT-1000). The tensile coupons were prepared and tested according to ACI 549.1R-93 [39]. The average properties of wire mesh such as modulus of elasticity, ultimate strength, and yield strength were 100 GPa, 600 MPa, and 405 MPa, respectively.

### 2.4. Epoxy Adhesive

Sikadur-31 was used as a structural adhesion material to attach the steel wire mesh to the surface of the concrete slab. It is free from solvent, moisture resistant, thixotropic, and the chemical base is an epoxy resin [61]. Sikadur-31 consists of two components: epoxy resins and special fillers that harden without shrinking. As per the manufacturer, the average compression, tensile, flexural, and bond strength are 75, 19, 30, and 4 MPa, respectively. These mechanical properties are obtained at 20 °C after seven days [61].

### 2.5. Strengthening Application

The all cast specimens were stripped from the molds after 24 h and immersed in a water tank for 28 days with almost constant laboratory temperature. Afterward, the specimens were taken out of the water for drying in air at laboratory conditions for three days. The area in which the epoxy was applied was cleaned and smoothed thoroughly to remove cement laitance, loose materials, and contaminants (i.e., dirt, oil, etc.) using an electric scraper machine. This preparation of the slab surface was made depending on the manufacturer's instructions for epoxy adhesive application [61]. After this step, the two components of the epoxy adhesive Sikadur-31 (A: white color and B: dark grey color) were mixed appropriately at 3: 1 proportions, using a slow speed electric drill. The mixing process continued until the mixture became homogenous in consistency and a uniform grey color [61]. Then, a film of the epoxy was applied to the tension surface of the concrete slabs. This thin layer of epoxy was used to seal small gaps on the surface of the prepared slabs, in order to fully ensure interconnectedness between the slab and strengthening layers. The bundle of four layers of steel wire mesh were tied together with a width equal to the slab thickness (95 mm), which was fixed mechanically to the concrete in its right place (Figures 2 and 3). The mixed epoxy adhesive was then applied to the layers of wire mesh that attached to the slab using a spatula tool with hand pressure to insure the epoxy adhesive reached to the slab and left no voids between the concrete slab and the wire mesh layers, in addition to no gaps between the mesh layers itself. The thickness of the epoxy adhesive layer was about 10 mm, as shown in Figure 2. This was done for the four sides of the column. The strengthened slabs were left for seven days in air at laboratory temperature before testing to ensure that the epoxy adhesive gained the final mechanical properties, as recommended in the manufacturer's instructions. Before testing, all slabs were painted using a white color emulsion paint so that the cracks could be seen well. The photos in Figure 3 show the arrangement and application procedure of the strengthening composites.

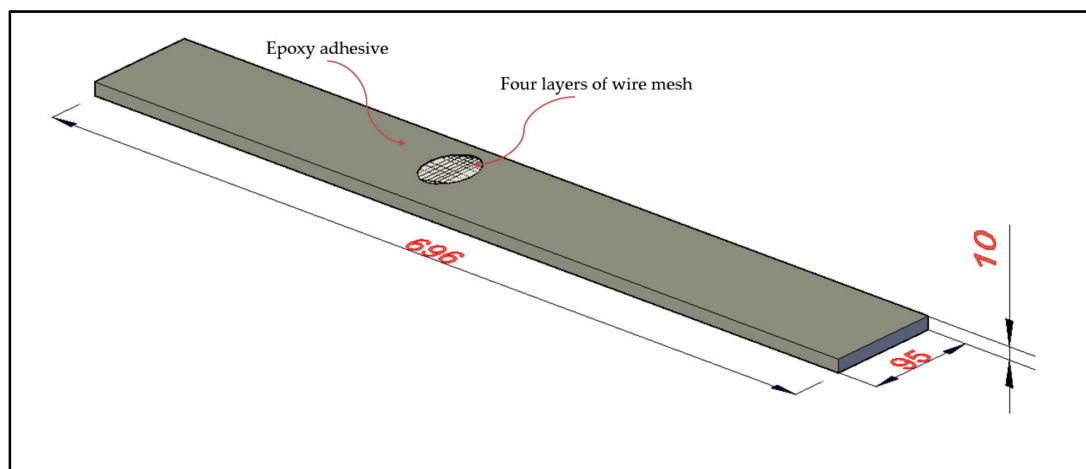


**Figure 2.** Details of the wire mesh-epoxy composite (unit: mm).

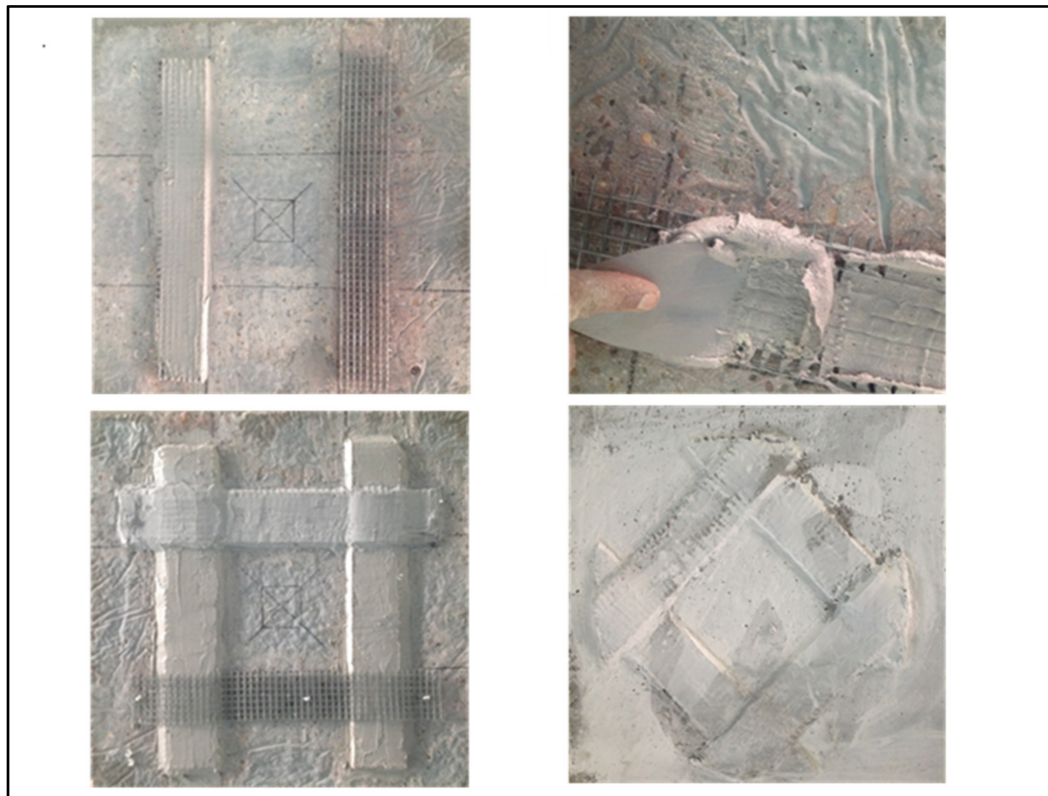


**Figure 3.** Application and arrangement of the strengthening composites.

### 3. Testing Procedure

The static axial concentrated load is applied at the center point of the slab specimens using a calibrated hydraulic piston testing machine of 250 kN, as shown in Figure 4. The used hydraulic jack was a load control type. The slab specimens rested along the four edges on a continuous 16 mm round bar (700 × 700 mm) in a two-way clear span condition, as shown in Figure 5. For adjustment and proper setting of the assembly, the specimens were preloaded with 2 kN. Then, the load application continued on the specimens in equal increments, starting from zero to failure. The under load central deflection was recorded for each load increment, using a dial gauge of 30 mm with 0.01 division placed directly at the center of the tension face of each slab. The slabs were supported with 700 mm of clear span. All specimens were subjected to a central single concentrated load that applied on the compressive face of the slab via a rigid steel plate with 80 × 80 × 40 mm dimensions. Crack patterns, modes of failure, and behavior of strengthening slabs were carefully observed throughout testing.

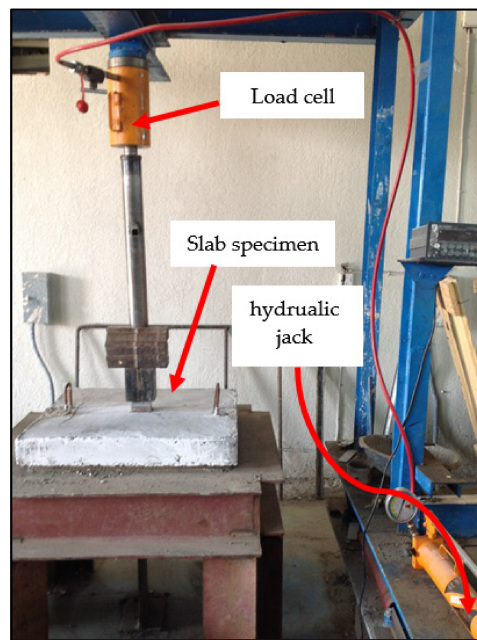


Figure 4. Test setup of the hydraulic piston testing machine.

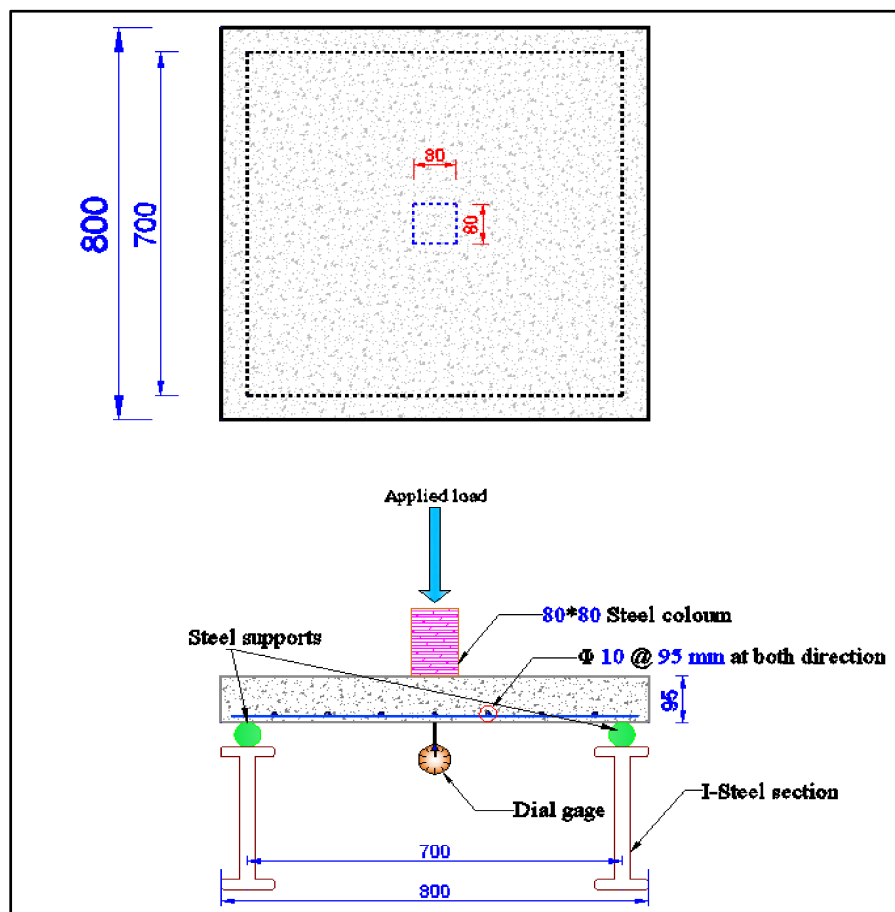


Figure 5. Loading and support condition of the test specimen (unit: mm).

### 4. Results and Discussions

#### 4.1. Load-Deflection Response

The load and deflection responses of the strengthened and reference specimens are demonstrated in Figures 6–8. As can be noticed from these figures, the load-deflection curves for the tested slabs ( $\rho = 1.15\%$ ) were comprised mainly of two parts. At the first loading stage, the first portion of the curves were nearly on a straight line, representing the flexural behavior of the specimens. After, the relationships exhibited a change in stiffness and the rate of deflection increased at the first cracking.

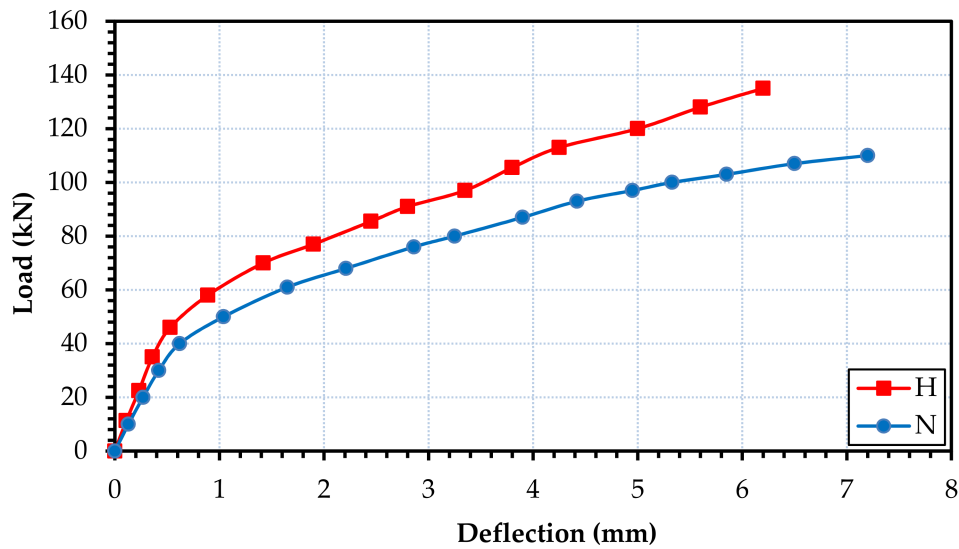


Figure 6. Effect of concrete compressive strength on punching load.

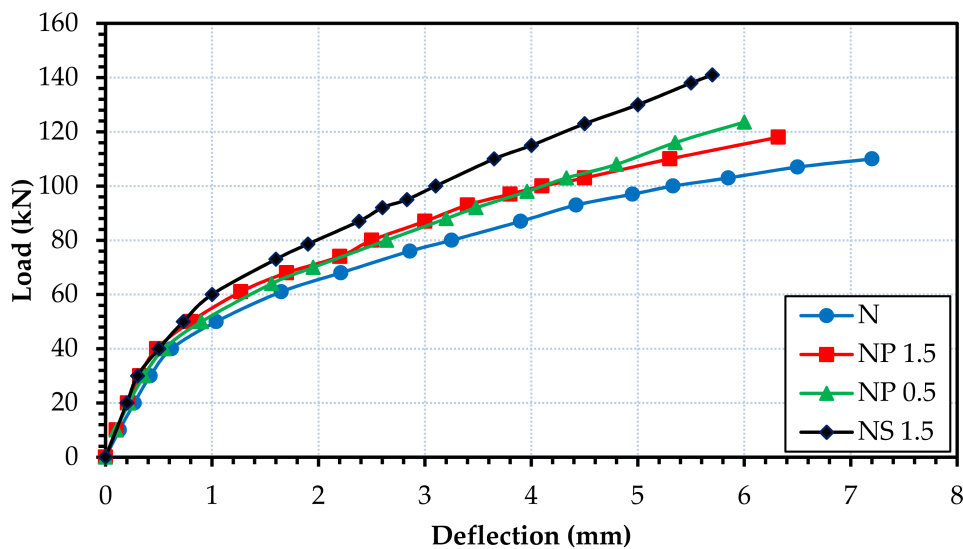


Figure 7. Strengthening effect of normal concrete slabs.

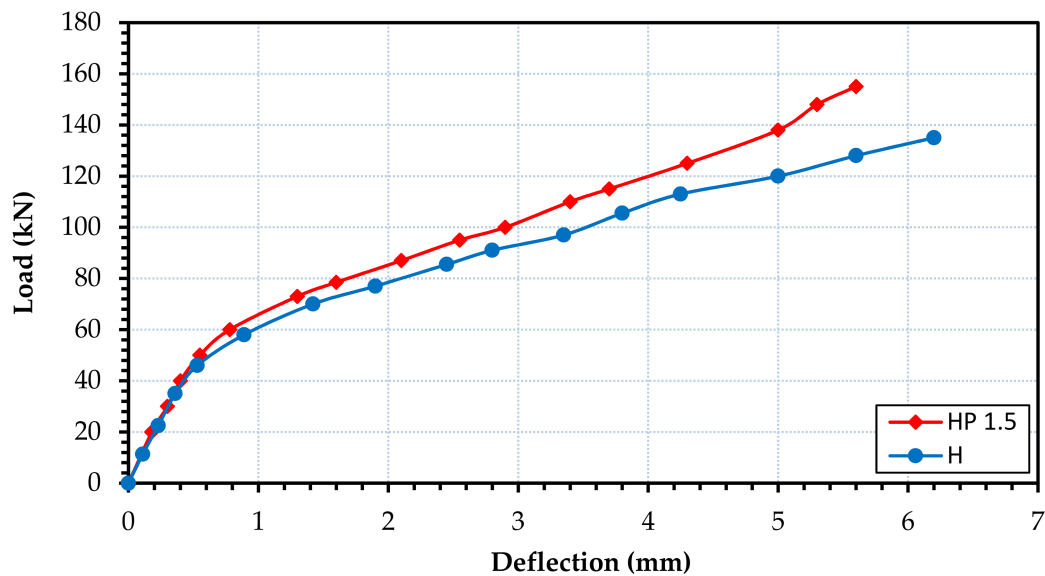


Figure 8. Strengthening effect on a high-strength concrete slab.

The stiffness of the slabs was lowered with an increase in the applied loads, which can be well observed after the initiation and development of the cracks. The first visible crack (the flexural crack) for the control specimens was observed at the tension side of the specimen, which was seen directly in the region under the loading point. When approaching maximum load, the load-deflection response appeared to significantly lower the stiffness of specimens and also showed that the curve of the load-deflection response is near a horizontal line. The maximum load reached 110 and 135 kN, with a corresponding average deflection of 7.2 and 6.2 mm, before failing in a punching shear for N and H specimens, respectively.

Each strengthened slabs experienced a negligible reduction in deflection until the first cracking stage, giving an indication of the insignificant increase in stiffness due to the attached strengthening composite (Figures 7 and 8). At the same time, the load remained the same for all specimens, indicating that no additional shear strength was achieved by strengthening the composite. On the other hand, the second portion of the curve reflected the brittle punching shear behavior of the slab, in which the increase in failure load and an accompanying reduction in deflection occurred for the strengthened slabs relative to the corresponding non-strengthened ones. This can be mainly attributed to the strengthening composite. Compared to Figures 7 and 8, the higher and steeper curve indicates the more efficient arrangement of strips when enhancing the slab behavior by restricting the formation of the failure mechanism. Accordingly, the skewed strengthening configuration has a more efficient performance among others, as it increased failure load by 28% and reduced corresponding deflection by 21%. It should be noted that the skewed strengthening pattern performs better than the orthogonal configuration. This may be due to the skewed orientation of the strengthening bundle located almost in an orthogonal direction of the extended radial cracks, which led to the intersection of developing crack growths. On the other hand, this may be returned to the internal steel reinforcement and the external reinforcement (skew configuration), were placed in different directions. The above reasons make the specimen NS 1.5 appear to have greater strength than specimen NP 1.5. In addition, the critical failure of the non-strengthened specimen N occurred at a distance of 88 mm from the face of the column, as presented in Table 5. This indicates that the distance was approximately  $1.5d$  from the face of the column. The presence of the strengthening strips close to this critical region helped intersect the propagation of cracks that appeared intensively in this area and prevented extended crack width. Further, it seems more efficient in its restriction of crack growth. This leads to the improvement of the carrying capacity of strengthened slab NS 1.5 over other models.

**Table 5.** Failure section parameters for the test slabs.

Test Slab	Effective Depth d (mm)	Measured Experimental Results			The Distance of Critical Punching Section from Column Face		
		Punching Failure Area (mm <sup>2</sup> )	Critical Failure Distance (x/2) <sup>(1)</sup>	Failure Angle $\phi$ <sup>(2)</sup>	ACI 318 d/2	BS 8110 1.5 d	CEB -1990 2 d
N	65	160,033	88	20.3			
NP 0.5	65	128,026	74	23.7			
NP 1.5	65	121,625	71	24.6			
NS 1.5	65	108,822	66	26.2	32.5	97.5	130
H	65	194,490	100	18.1			
HP 1.5	65	161,425	86	20.7			

ACI Committee 318: Building code requirements for structural concrete and commentary. ACI 318-11/ACI 318R-11. American Concrete Institute: Farmington Hills, MI: 2011. p. 503; BS 8110: Structural Use of Concrete—Part 1: Code of Practice for Design and Construction, 1997. (London); CEB-FIP MC-1990: “Comité Euro-International Du Béton-Fédération de la Précontrainte”, Final draft, Model Code, Bulletin d’information, Lausanne, Switzerland, No. 203, 1991, p. 462; <sup>(1)</sup> Calculated according to failure model Figure 11; <sup>(2)</sup>  $\phi = \tan^{-1}(d/x)$ .

The effect of the compressive strength of concrete on punching shear capacity can be observed in Figure 6 and the data listed in Table 1. From this figure, an increase is noticed in the failure load of 22.7%, as the concrete compressive strength increases from 30 to 65 MPa.

#### 4.2. Modes of Failure

Generally, all test specimens experienced the same stress due to the application of the central concentrated load, featuring the creation of flexural, diagonal, and radial cracks that propagated from the under-load point towards the specimens supported edges. Next, the crack mode became circular, as the load reached a higher value, altering the gradual flexural behavior to the rapid sudden (brittle) shear failure, as shown clearly by the load-deflection curves in Figures 6–8. The pyramid failure shape was the same for all specimens, with only a difference of change in the failure area at the tension side, due to the different strengthening effect on the failure cracks. The pyramid concrete mass split from the slab together with the strengthening strips without any debonding evidence, as shown in Figure 9. The failure mode for all tested specimens was the punching failure mode; the punching area of strengthened specimens was smaller than the control slabs. Moreover, the punching failure of the strengthened specimens consequently led to the delamination of the wire mesh-epoxy composite, as can be seen in Figure 9. Figure 10 demonstrates specimen NP 1.5 before and after the removal of strengthening strips from the tension side of slab after failure. It is clearly shown that the large parts of the concrete remained fully attached with the strengthening strips after the reinforcement system was removed. This proves that no debonding occurs between the slabs and strengthening materials.

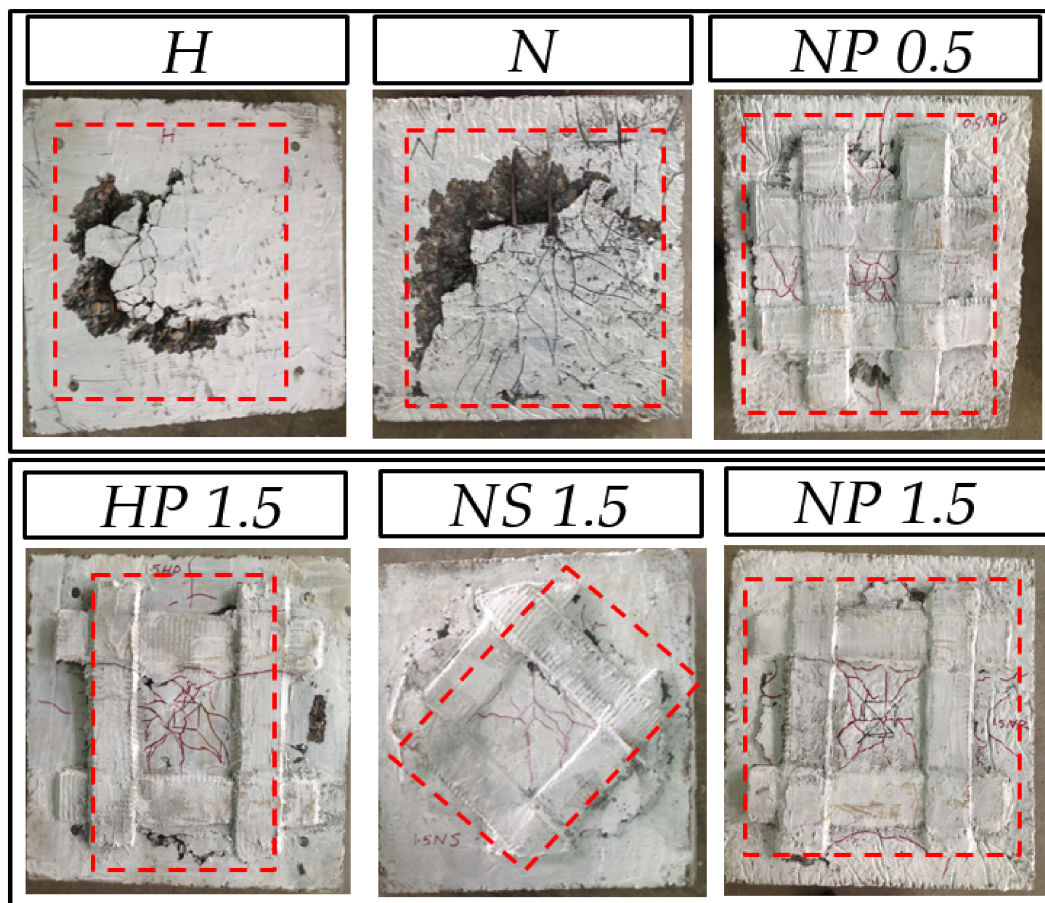


Figure 9. Failure mode and crack patterns of the tested specimens.

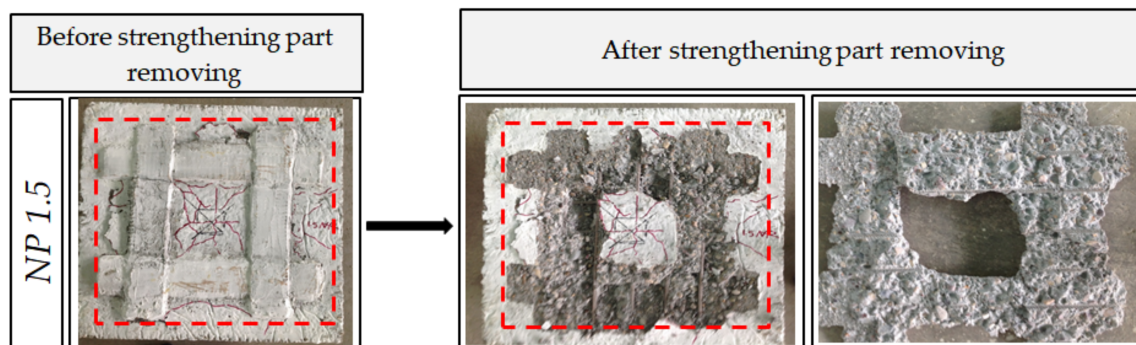
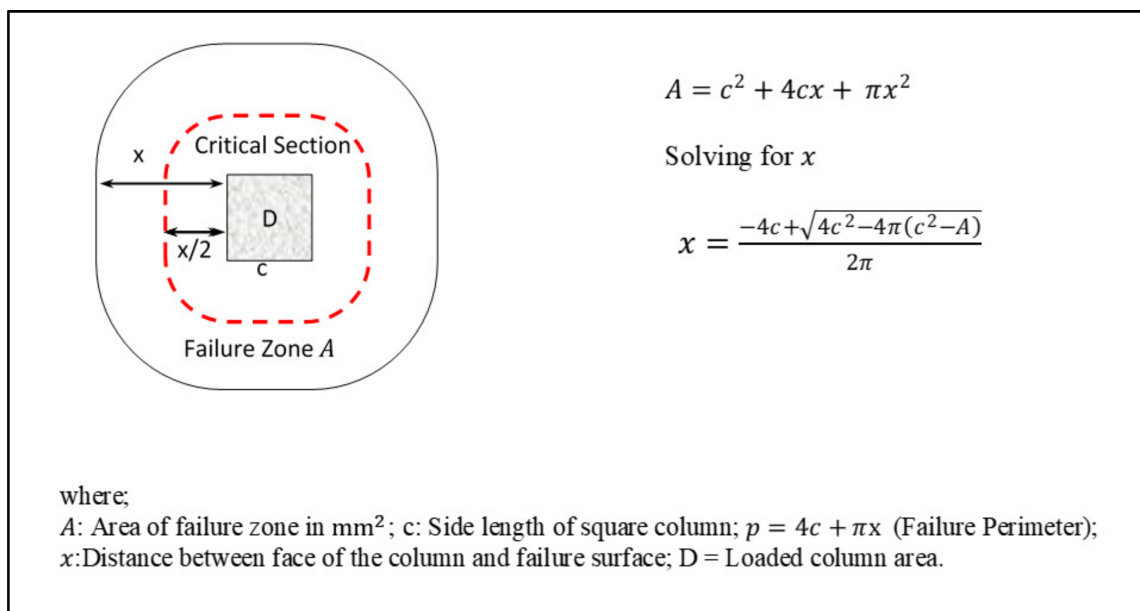


Figure 10. Failure mode before and after the strengthening part was removed from the tested specimens.

#### 4.3. Critical Section Perimeters

In the current study, the area enclosed by the failure surface included the perimeters and failure angle of the failure zone, which was measured experimentally. The value of ( $x$ ) represents the distance from the column's face to the edge of the failure zone, which was determined according to the failure model, as shown in Figure 11. This mode was adopted by European Code [62], which considered the punched failure area "A" as a sum of (1) the column area ( $c^2$ ), (2) four areas of  $C.x$ , and (3) four areas of  $\pi x^2/4$ . It is important to consider that the critical punching shear section is half of this distance ( $0.5 x$ ). Table 5 shows the values obtained from the test specimens compared to the values adopted by a different code of practice.



**Figure 11.** Failure model used to calculate the critical sections as presented in European code (modified from [62]).

Based on the measured failure area of the tested specimens listed in Table 5, the distance and failure angle of the corresponding critical shear failures was obtained using the failure model shown in Figure 11. The results showed an increase of 21% in the failure area of the high strength concrete. This is compared to the normal strength, where it showed a decrease of 20% to 32% in the failure area and a higher value was found in the skewed strengthening configuration. The reduction was only 17% in high-strength concrete. The changes in the failure distances ( $x$ ) and the angles of failure ( $\phi$ ) are related to the changes in the failure area, where  $x$  follows the same trend and  $\phi$  takes the opposite. In comparison with the codes of practice, the values of the failure distances  $x$  are between  $d$  at the skewed strengthened slab and  $1.5 d$  in high-strength concrete slabs.

Punching shear strength at the failure perimeter of the tested slabs was determined using the failure model and its related equations, compared to those determined by the codes of practice. Although these values are higher than that of the codes, they are still lower than the limit value of BS 8110, which is less than  $0.8\sqrt{f_{cu}}$  or 5 MPa allowed for members subjected to shear enhancement process. Table 6 shows that the highest shear strength value occurs at the skewed strengthened slab, where the failure perimeter has the lowest length. As mentioned in the previous section, this is due to the contribution of the skewed strengthening in limiting and ending the propagation of the early starting diagonal cracks. In this case, the load is 141 kN divided by the failure cross section, which is the product of the perimeter ( $4 \times 80 + 132 \pi$ ) of the punched area, multiplied by the effective depth  $d$  (65).

**Table 6.** Ultimate load and shear strength comparison.

Test Slab	Concrete Comp. Strength (MPa)	Effective Depth (mm)	Ultimate Load (kN)	Perimeter of Punched Area (*) (mm)	Ultimate Punching Shear Strength (MPa)	ACI 318 (V) <sup>(1)</sup> (kN) (V)MPa	BS 8110 (V) <sup>(2)</sup> (kN) (V)MPa	CEB-90 (V) <sup>(3)</sup> (kN) (V)MPa
N	30	65	110	873	1.94			
NP 0.5	30	65	124	785	2.42	(60.2)	(99)	(85.5)
NP 1.5	30	65	118	766	2.37	<b>1.60</b>	<b>1.4</b>	<b>1.16</b>
NS 1.5	30	65	141	735	2.95			
H	65	65	135	945	2.20	(88.6)	(128)	(110.6)
HP 1.5	65	65	155	860	2.77	<b>2.35</b>	<b>1.8</b>	<b>1.50</b>

(\*)  $p = 4c + \pi x$ ; (1)  $V_c = 0.33 \sqrt{f'c} bo d$ ; (2)  $V_c = 0.79 (100\rho)^{\frac{1}{3}} \left(\frac{400}{d}\right)^{\frac{1}{4}} (f_{cu}/25)^{\frac{1}{3}} bo d$ ; (3)  $V_c = 0.18 k (100 \rho f'c)^{\frac{1}{3}} bo d$ . Where  $p$  is perimeter of punched area (mm);  $c$  is the side length of the square column (mm);  $x$  is the distance between the face of the column and the failure surface (mm);  $V_c$  is the ultimate punching shear strength (kN);  $d$  is the effective depth of slab (mm);  $bo$  is the length of perimeter at the critical section (mm);  $\rho$  is the reinforcement ratio;  $f'c$  is the concrete compressive strength of the cylinder (MPa);  $f_{cu}$  is the concrete compressive strength of cube (MPa); and  $k = 1 + \left(\frac{200}{d}\right)^{\frac{1}{2}}$  is the size-effect coefficient.

**4.4. Ductility Index and Ultimate Reserve Shear**

The values of shear ductility index, defined as  $\left(\mu = \frac{\Delta_u}{\Delta_{cr}}\right)$ , for the tested slabs, are shown in Table 7. From this table, it can be noticed that the ductility index for both types of concrete strength specimens are approximately the same, wherein all strengthened specimens featured a loss in ductility. The skewed strengthening configuration specimen NS displayed a 1.7% loss in ductility, compared with the non-strengthened one of the same concrete grade. There was a 6% and 4% loss for NP 0.5 and NP 1.5, respectively. Ultimately, the drop was 13% in strengthened high strength concrete HP 1.5 specimen. This loss in ductility was due to the restriction of formation of the flexural failure mechanism added by the strengthening composite, which resulted in a reduction of the deflection value, at which the shear failure began occurring at the ultimate failure point.

**Table 7.** Shear ductility index and ultimate reserve shear.

Test Slab	$\Delta_u$ mm	$V_u$ kN	Shear Ductility Index $\mu = \frac{\Delta_u}{\Delta_{cr}}$	Reserve Shear $\left(\frac{V_u - V_{cr}}{V_{cr}}\right)\%$
N	7.2	110	11.6	175
NP 0.5	6.0	124	10.9	209
NP 1.5	6.3	118	11.1	195
NS 1.5	5.7	141	11.4	252
H	6.2	135	11.7	193
HP 1.5	5.6	155	10.2	210

The cracking and maximum shear for all specimens is summarized in Table 7. The ratio value  $\left(\frac{V_u}{V_{cr}}\right)$  can be used as a measure to reserve shear strength beyond creation of the first diagonal crack, which can be considered as a warning signal indicator. From this table, it can be seen that the specimens strengthened with wire mesh-epoxy composites led to enhanced reserve shear strength. However, the reserve shear ratio  $\left(\frac{V_u - V_{cr}}{V_{cr}}\right)\%$  compared with the control slab were 11%, 20%, and 44% for slabs NP 1.5, NP 0.5, and NS 1.5 made with normal strength, respectively. This ratio was 8% for the high strength slab HP 1.5. This increase in shear reserve returns to the effect of strengthening materials. Moreover, for the same compressive strength for strengthened slabs, the skew configurations appeared to have a higher efficiency in shear capacity. For the specimens NP 1.5 and HP 1.5, which were strengthened with the same configuration and different concrete compressive strength, the shear reserve slightly increased with the concrete strength.

## 5. Conclusions

The main conclusions drawn from this study can be summarized as follows:

1. This new technique of using a composite of steel wire mesh fully coated with epoxy and externally attaching it to the slab surface was found as an effective, easy, and practical way of strengthening reinforced concrete flat plates and enhancing their capacity against punching shear failure.
2. The strengthening composite did not alter the mode of failure, which indicates that the same principles, assumptions, and failure criteria can be extended to formalize the enhancing achievement. No debonding occurred between the strengthened materials and slabs.
3. All types of strengthening composite configurations achieved an incremental increase in the ultimate punching shear load capacity and a decrease in the corresponding failure deflection.
4. The maximum increase in the punching shear load capacity was 28%. Further, a minimum load deflection was achieved by the skewed strengthening configuration; it was 7% for the parallel at 1.5 d slab.
5. Although the ultimate shear stress at the critical sections of the strengthened slabs increased to a maximum value of 2.95 MPa, it is well below the limits of BS 8110.
6. The maximum drop in ductility was experienced by the high strength concrete slab (13%). Further, the minimum (1.7%) was experienced by the skewed strengthened normal concrete slab.
7. The 45° skewed configuration strengthening composite was the most efficient among the strengthened slabs investigated in this study. The maximum percentage of reserve shear attained by this configuration increased to 44% compared with the reference slab.

**Author Contributions:** Conceptualization, A.A.J., and R.A.; methodology, A.A.J. and R.A.; validation, A.A.J. and R.A.; investigation, A.A.J.; resources, A.A.J.; data curation, A.A.J.; writing-original draft preparation, R.A.; writing-review and editing, A.A.J., R.A., and S.L.K.; visualization, A.A.J., R.A., and S.L.K.; Software, S.L.K.; project administration, S.L.K.

**Funding:** This research received no external funding.

**Acknowledgments:** The authors would like to thank University of Misan-College of Engineering-Civil Engineering Departments for facilities and assistance throughout this study.

**Conflicts of Interest:** The authors declare that there is no conflict of interests regarding the publication of this paper.

## References

1. Youm, K.S.; Kim, J.J.; Moon, J. Punching shear failure of slab with lightweight aggregate concrete (LWAC) and low reinforcement ratio. *Constr. Build. Mater.* **2014**, *65*, 92–102. [[CrossRef](#)]
2. Elsanadedy, H.M.; Al-Salloum, Y.A.; Alsayed, S.H. Prediction of punching shear strength of HSC interior slab-column connections. *KSCE J. Civ. Eng.* **2013**, *17*, 473–485. [[CrossRef](#)]
3. Osman, M.; Marzouk, H.; Helmy, S. Behavior of high-strength lightweight concrete slabs under punching loads. *ACI Struct. J.* **2000**, *97*, 492–498.
4. Macdonald, M.; Calder, A. Bonded steel plating for strengthening concrete structures. *Int. J. Adhes. Adhes.* **1982**, *2*, 119–127. [[CrossRef](#)]
5. Meisami, M.H.; Mostofinejad, D.; Nakamura, H. Punching shear strengthening of two-way flat slabs using CFRP rods. *Compos. Struct.* **2013**, *99*, 112–122. [[CrossRef](#)]
6. Thanoon, W.A.; Jaafar, M.; Kadir, M.R.A.; Noorzai, J. Repair and structural performance of initially cracked reinforced concrete slabs. *Constr. Build. Mater.* **2005**, *19*, 595–603. [[CrossRef](#)]
7. Martinez-Cruzado, J.; Qaisrani, A.; Moehle, J. Post-tensioned flat plate slab-column connections subjected to earthquake loading. In Proceedings of the 5th US National Conference on Earthquake Engineering, Chicago, IL, USA, 10–14 July 1994; pp. 139–148.
8. Hassanzadeh, G.; Sundquist, H. Strengthening of bridge slabs on columns. *Nord. Concr. Res. Publ.* **1998**, *21*, 23–34.
9. Polak, M.A. Ductility of Reinforced Concrete Flat Slab-Column Connections. *Comput. Aided Civ. Infrastruct. Eng.* **2005**, *20*, 184–193. [[CrossRef](#)]

10. Ruiz, M.F.; Muttoni, A.; Kunz, J. Strengthening of Flat Slabs against Punching Shear Using Post-Installed Shear Reinforcement. *ACI Struct. J.* **2010**, *107*, 434–442.
11. Farhey, D.N.; Adin, M.A.; Yankelevsky, D.Z. Repaired RC Flat-Slab-Column Subassemblages under Lateral Loading. *J. Struct. Eng.* **1995**, *121*, 1710–1720. [[CrossRef](#)]
12. Raithby, K.D. Strengthening of concrete bridge decks with epoxy-bonded steel plates. *Int. J. Adhes. Adhes.* **1982**, *2*, 115–118. [[CrossRef](#)]
13. Meier, U. Strengthening of structures using carbon fibre/epoxy composites. *Constr. Build. Mater.* **1995**, *9*, 341–351. [[CrossRef](#)]
14. Bakis, C.; Davalos, J.F.; Lesko, J.J.; Machida, A.; Rizkalla, S.H.; Triantafillou, T.; Bank, L.C.; Brown, V.L.; Cosenza, E. Fiber-Reinforced Polymer Composites for Construction—State-of-the-Art Review. *J. Compos. Constr.* **2002**, *6*, 73–87. [[CrossRef](#)]
15. Li, H.; Wang, W.; Zhou, W. Fatigue damage monitoring and evolution for basalt fiber reinforced polymer materials. *Smart Struct. Syst.* **2014**, *14*, 307–325. [[CrossRef](#)]
16. Ju, M.; Park, K.; Park, C. Punching Shear Behavior of Two-Way Concrete Slabs Reinforced with Glass-Fiber-Reinforced Polymer (GFRP) Bars. *Polymer* **2018**, *10*, 893. [[CrossRef](#)] [[PubMed](#)]
17. Smith, S.T.; Hu, S.; Kim, S.J.; Seracino, R. FRP-strengthened RC slabs anchored with FRP anchors. *Eng. Struct.* **2011**, *33*, 1075–1087. [[CrossRef](#)]
18. Sundarraja, M.; Rajamohan, S.; Bhaskar, D. Shear Strengthening of RC Beams Using GFRP Vertical Strips—An Experimental Study. *J. Reinf. Plast. Compos.* **2008**, *27*, 1477–1495. [[CrossRef](#)]
19. Erki, M.; Heffernan, P. Reinforced concrete slabs externally strengthened with fibre-reinforced plastic materials. In Proceedings of the second international RILEM symposium FRPRCS-2, Belgium, Ghent, 23–25 August 1995; pp. 209–516.
20. Kheyroddin, A.; Vaez, S.R.H.; Naderpour, H. Numerical Analysis of Slab-Column Connections Strengthened with Carbon Fiber Reinforced Polymers. *J. Appl. Sci.* **2008**, *8*, 420–431.
21. Harajli, M.H.; Soudki, K.A. Shear Strengthening of Interior Slab-Column Connections Using Carbon Fiber-Reinforced Polymer Sheets. *J. Compos. Constr.* **2003**, *7*, 145–153. [[CrossRef](#)]
22. El-Salakawy, E.; Soudki, K.A.; Polak, M.A. Punching Shear Behavior of Flat Slabs Strengthened with Fiber Reinforced Polymer Laminates. *J. Compos. Constr.* **2004**, *8*, 384–392. [[CrossRef](#)]
23. Harajli, M.H.; Soudki, K.A.; Kudsi, T. Strengthening of Interior Slab-Column Connections Using a Combination of FRP Sheets and Steel Bolts. *J. Compos. Constr.* **2006**, *10*, 399–409. [[CrossRef](#)]
24. Wang, J. *Punching Shear Behaviour of RC Flat Plates Externally Strengthened with FRP Systems*; National University of Singapore: Singapore, 2002.
25. Sharaf, M.H.; Soudki, K.A.; Van Dusen, M. CFRP Strengthening for Punching Shear of Interior Slab-Column Connections. *J. Compos. Constr.* **2006**, *10*, 410–418. [[CrossRef](#)]
26. Soudki, K.A.; El-Sayed, A.K.; Vanzwol, T. Strengthening of concrete slab-column connections using CFRP strips. *J. King Saud Univ. Eng. Sci.* **2012**, *24*, 25–33. [[CrossRef](#)]
27. Chiew, S.P.; Sun, Q.; Yu, Y. Flexural Strength of RC Beams with GFRP Laminates. *J. Compos. Constr.* **2007**, *11*, 497–506. [[CrossRef](#)]
28. Grace, N.F.; Sayed, G.A.; Soliman, A.K.; Saleh, K.R. Strengthening reinforced concrete beams using fiber reinforced polymer (FRP) laminates. *ACI Struct. J. Am. Concr. Inst.* **1999**, *96*, 865–874.
29. Ritchie, P.A.; Thomas, D.A.; Lu, L.W.; Connely, G.M. External Reinforcement of Concrete Beams Using Fiber Reinforced Plastic. *ACI Struct. J.* **1991**, *88*, 490–500.
30. Toutanji, H.; Zhao, L.; Zhang, Y. Flexural behavior of reinforced concrete beams externally strengthened with CFRP sheets bonded with an inorganic matrix. *Eng. Struct.* **2006**, *28*, 557–566. [[CrossRef](#)]
31. Triantafillou, T.C.; Plevris, N.; Triantafillou, T. Strengthening of RC beams with epoxy-bonded fibre-composite materials. *Mater. Struct.* **1992**, *25*, 201–211. [[CrossRef](#)]
32. Sharif, A.; Al-Sulaimani, G.J.; Basunbul, I.A.; Baluch, M.H.; Ghaleb, B.N. Strengthening of Initially Loaded Reinforced Concrete Beams Using FRP Plates. *ACI Struct. J.* **1994**, *91*, 160–168.
33. Gose, S.; Nanni, A.J.R. *Anchorage System for Externally Bonded FRP Laminates Using Near Surface Mounted Rods*; Centre for Infrastructure Engineering Studies, University of Missouri-Rolla: Rolla, MI, USA, 2000.
34. Smith, S.T.; Teng, J.-G. Shear-Bending Interaction in Debonding Failures of FRP-Plated RC Beams. *Adv. Struct. Eng.* **2003**, *6*, 183–199. [[CrossRef](#)]

35. Wu, Y.-F.; Huang, Y. Hybrid Bonding of FRP to Reinforced Concrete Structures. *J. Compos. Constr.* **2008**, *12*, 266–273. [[CrossRef](#)]
36. Al-Mahaidi, R.; Kalfat, R. Investigation into CFRP laminate anchorage systems utilising bi-directional fabric wrap. *Compos. Struct.* **2011**, *93*, 1265–1274. [[CrossRef](#)]
37. Koutas, L.N.; Bournas, D.A. Flexural strengthening of two-way RC slabs with textile-reinforced mortar: Experimental investigation and design equations. *J. Compos. Constr.* **2016**, *21*, 04016065. [[CrossRef](#)]
38. Abbaszadeh, M.A.; Sharbatdar, M.K.; Kheyroddin, A. Performance of Two-way RC Slabs Retrofitted by Different Configurations of High Performance Fibre Reinforced Cementitious Composite Strips. *Open Civ. Eng. J.* **2017**, *11*, 650–663. [[CrossRef](#)]
39. ACI Committee 549. Guide for the design, construction, and repair of ferrocement. *ACI Struct. J.* **1988**, *85*, 325–351.
40. Kondraivendhan, B.; Pradhan, B. Effect of ferrocement confinement on behavior of concrete. *Constr. Build. Mater.* **2009**, *23*, 1218–1222. [[CrossRef](#)]
41. Fahmy, E.; Shaheen, Y. Laminated ferrocement for strengthening and repairing of reinforced concrete beams. In Proceedings of the Annual Conference of the Canadian Society for Civil Engineering, Winnipeg, MB, Canada, 1–4 June 1994; pp. 475–483.
42. Fahmy, E.; Shaheen, Y.; Korany, Y.S. Repairing reinforced concrete columns using ferrocement laminates. *J. Ferrocem.* **1999**, *29*, 115–124.
43. Shannag, M.J. High strength ferrocement laminates for structural repair. In *Concrete Solutions*; CRC Press: Boca Raton, FL, USA, 2009; pp. 385–388.
44. Jeyasehar, C.; Vidivelli, B. Behaviour of RC beams rehabilitated with ferrocement laminate. In Proceedings of the Eight International Symposium and Workshop on Ferrocement and Thin Reinforced Cement Composites, Bangkok, Thailand, 6–8 February 2006; pp. 485–500.
45. Lub, K.; Van Wanroij, M.J.J.o.f. Strengthening of reinforced concrete beams with shotcrete-ferrocement. *J. Ferrocem.* **1989**, *19*, 363–371.
46. Paramasivam, P.; Lim, C.; Ong, K. Strengthening of RC beams with ferrocement laminates. *Cem. Concr. Compos.* **1998**, *20*, 53–65. [[CrossRef](#)]
47. Dongyen, A.; Sayanamipuk, S.; Piyarakshul, S.; Nimityongskul, P. Strengthening of reinforced concrete beam and slab system using ferrocement jacketing. In Proceedings of the Eight International Symposium and Workshop on Ferro Cement and Thin Reinforced Cement Composites, Bangkok, Thailand, 6–8 February 2006; pp. 461–472.
48. Naaman, A.E. *Ferrocement and Laminated Cementitious Composites*; Techno Press: Ann Arbor, MI, USA, 2000; Volume 3000.
49. El Debs, M.; Naaman, A. Bending behavior of mortar reinforced with steel meshes and polymeric fibers. *Cem. Concr. Compos.* **1995**, *17*, 327–338. [[CrossRef](#)]
50. Shannag, M.J.; Bin Ziyad, T. Flexural response of ferrocement with fibrous cementitious matrices. *Constr. Build. Mater.* **2007**, *21*, 1198–1205. [[CrossRef](#)]
51. Ibrahim, H.M.J.C.; Materials, B. Experimental investigation of ultimate capacity of wired mesh-reinforced cementitious slabs. *Constr. Build. Mater.* **2011**, *25*, 251–259. [[CrossRef](#)]
52. Kaish, A.; Jamil, M.; Raman, S.; Zain, M.; Nahar, L. Ferrocement composites for strengthening of concrete columns: A review. *Constr. Build. Mater.* **2018**, *160*, 326–340. [[CrossRef](#)]
53. Li, X.; Xie, H.; Yan, M.; Gou, H.; Zhao, G.; Bao, Y. Eccentric Compressive Behavior of Reinforced Concrete Columns Strengthened Using Steel Mesh Reinforced Resin Concrete. *Appl. Sci.* **2018**, *8*, 1827. [[CrossRef](#)]
54. Qeshta, I.M.; Shafigh, P.; Jumaat, M.Z.; Abdulla, A.I.; Ibrahim, Z.; Alengaram, U.J. The use of wire mesh-epoxy composite for enhancing the flexural performance of concrete beams. *Mater. Des.* **2014**, *60*, 250–259. [[CrossRef](#)]
55. Qeshta, I.M.; Shafigh, P.; Jumaat, M.Z.; Abdulla, A.I.; Alengaram, U.J.; Ibrahim, Z. Flexural behaviour of concrete beams bonded with wire mesh-epoxy composite. In *Applied Mechanics and Materials*; Trans Tech Publications: Zurich, Switzerland, 2014; pp. 411–416.
56. Qeshta, I.M.; Shafigh, P.; Jumaat, M.Z. Flexural behaviour of RC beams strengthened with wire mesh-epoxy composite. *Constr. Build. Mater.* **2015**, *79*, 104–114. [[CrossRef](#)]
57. *Iraqi Specification No.5/1984, "Portland Cement"*; Central Organization for Standardization and Quality Control: Baghdad, Iran, 2001.

58. ACI 211.1-91 Cmmittee. *Standard Practice for Selecting Proportions for Normal, Heavyweight, and Mass Concrete*; ACI Manual of Concrete Practice, Part 1; American Concrete Institute: Detroit, MI, USA, 1991; pp. 211.1-1–211.1-38.
59. ACI 211.4R-93 Cmmittee. Guide for selecting proportions for high-strength concrete with Portland cement and fly Ash. *ACI Mater. J.* **1993**, *90*, 272–283.
60. ASTM, S.J.A.A.M.-b. *Standard Specification for Deformed and Plain Carbon-Steel Bars for Concrete Reinforcement*; A615/A615M-09; ASTM International: West Conshohocken, PA, USA, 2009.
61. *Sika Product Data Sheet, Sikadur®-31 CF Normal, Product Data Sheet, 2-Components Thixotropic Epoxy Adhesive*; Sika Product Data Sheet. Sika Group: Watchmead, Welwyn Garden City, UK, 2013; Volume 2031. Available online: [https://gbr.sika.com/en/solutions\\_products/sika-markets/structural-strengthening/products-andsystems/02a013sa04.html](https://gbr.sika.com/en/solutions_products/sika-markets/structural-strengthening/products-andsystems/02a013sa04.html) (accessed on 21 July 2019).
62. *CEB-FIP MC-1990*; Final draft, Model Code, Bulletin d’information; Comité Euro-International Du Béton-Fédération de laPrécontrainte: Lausanne, Switzerland, No. 203; 1991; p. 462.



© 2019 by the authors. Licensee MDPI, Basel, Switzerland. This article is an open access article distributed under the terms and conditions of the Creative Commons Attribution (CC BY) license (<http://creativecommons.org/licenses/by/4.0/>).